Synthesis and characterization of S−IPN hydrogels of chitosan/PVA/PNIPAm to be used in the design of nucleus pulpous prosthesis

Marcos Antonio Sabino[1*]; Reinaldo Aandres Garcia[1]

Corresponding author: e−mail address: msabino@usb.ve

Abstract: Hydrogels (HG) have been widely used in biomedical applications due to their high−water content which improves their biocompatibility with living tissue. In this study, Chitosan (CS) hydrogels cross−linked with Genipin and semi interpenetrated network (S−IPN) with PVA/PNIPAm were prepared to be used in the design of nucleus pulpous (NP) prosthesis. Chemical structure, morphology, swelling ratio (SR), mechanical properties and cytotoxicity were evaluated through a variation of the Genipin percentage and CS/PVA/PNIPAm proportions. Those experiments were carried out through Fourier−Transform Infrared Spectroscopy, Scanning Electron Microscopy, swelling studies, dynamic rheology, and hemocompatibility tests. The results showed that regardless of the Genipin percentage or polymers proportions, all HGs had interconnected porous structure, and change microstructurally, the pore size, its size distribution and the wall thickness. Firstly, an increment in the Genipin percentage and in the CS proportion concluded in an augmentation of the pore size. Secondly, an augmentation in the PVA proportion ended up producing smaller pores, with larger wall thickness and more homogeneous pore size distribution. The variation in PNIPAm proportion didn´t influence the morphology, but did have an impact on the SR and storage modulus (G´) augmenting in both cases as the PNIPAm proportion. The swelling ratio turned out to be related to the pore morphology; as smaller the pore size, smaller the SR. Likewise, the storage modulus rose insofar the SR diminished. In these S−IPN HGs, G´ varied between 77 Pa and 27000 Pa, values below and above G´ reported for human NP. Also, δ varied between 1.4° and 13.17° while the δ reported for NP is 23°−31°. Finally, the hemocompatibility tests did not show cellular lysis for any formulation. These outcomes demonstrated that from the rheological and hemocompatibility point of view, this kind of as semi interpenetrated networks (S−IPNs) HGs can be tailored to attain the NP´s properties.

Keywords: Chitosan. PVA. PNIPAm. Genipin. LCST. δ. Storage modulus. S−IPN and Hydrogel.

Introduction

The vertebral spine is the structure responsible for providing support to the body and protecting the spinal cord. The structure is linked by 24 mobile vertebral bones, 7 of them in the cervical region, 12 in the thoracic region and 5 in the lumbar region. This latter region is the one that withstands most of the load with up to the 55% of all the load produced by the body mass [1, 2]. The intervertebral discs (IVD) are embedded between those vertebral bodies and macroscopically, are composed by the nucleus pulpous (NP) surrounded by the annulus fibrous and on the top and bottom of NP (and part of the AF) you will find the endplates[3, 4].

The NP is a fibro cartilaginous material, with a water content that varies from 90% (at birth) to 70% or less at the age of 60 years old[5]. This amount of water in the NP allows its deformation while maintaining an incompressible volume. Thus, when a pressure is applied from above, the NP reduces its height and attempts to expand radially (which is prevented by the AF). Therefore, the NP transmits the pressure outwards towards the collagen fibers in the annulus, which stores and absorbs the energy developing tension. NP and AF bear part of the load, the rest is transmitted through the vertebral endplates to the next vertebra. When the load ceases, the stored energy in the collagen fibers is released and exerted back to the NP where it is used to restore any deformation[6]. This combined action of the NP and AF also endows the disc with a great resilience that acts as a shock absorber, lessening the speed transmission of forces from one vertebra to the other[3, 6, 7].

After water, the most abundant component of the NP are the proteoglycans with a content of 65% of the dry weight, which decreases up to 30% with aging[5]. These are hydrophilic molecules accountable for the content of water and for the generation of the osmotic pressure[2, 8].

Now, focusing on the specific case of low back pain (LBP), this can be generated by aging and diseases. The first one is a natural process that evokes changes in the extracellular matrix structure (which alter the synthetic capabilities of the disc cells) and increases the accumulation of degraded products that ultimately result in tissue degeneration[9]. On the other hand, degenerative disc disease (DDD) is the main source of chronic and recurring LBP, a condition that 80% of the population suffer in some part of their lives[10]. This syndrome alters the biomechanics of the disc, decreasing the proteoglycans content, dehydrating and shrinking the NP causing a reduction in the osmotic pressure resulting in an increased range of motion[1,11−14]. Once the NP is damaged, it suffers an increment in the shear modulus and a diminution of the swelling pressure, the relative energy dissipation, and the water content leading to a lessening of the height of the IVD. In extreme cases of failure or total removal of NP, excessive bulge of the AF layers leads to a collapse of the IVD[4,15,16].

Both aging and DDD can be developed even faster by adverse biomechanical loadings, overloads, loads borne for long times, bad postures and high impacts on the spine[4,17,18]. Studies have estimated the annual work productivity losses for LBP in the UK, Australia and USA in 9.1 billion £, 8.1 billion AUD$ and 100billion USD respectively[18−20].

Surprisingly, the most common approach to treat chronic low back diseases is to eliminate or di minish the pain rather than restoring the segment biomechanics[3,4]. When conservative treatments to relieve LBP (like heat and cold therapy, steroid injections, medication, physical therapy, etc.) do not work, surgical interventions are required. The most common surgical procedure in these cases is the intervertebral fusion. This treatment, despite diminishing pain, results in increased stiffness, loss of motion, and altered patterns of stress flow that produce altered biomechanics at adjacent motion segments[21−23].The second most common surgical treatment is the NP discectomy, but in the same way, this

one greatly alters the biomechanical function of the disc leading to further disc degeneration in the form of circumferential tears in the AF[1,24,25]. Furthermore, after discectomy, the NP space is filled with air, causing larger displacement because air is easily compressed[7,26]. Since these traditional treatments alter the segment biomechanics increasing the risks for adjacent segments degeneration in up to 35% and 45%, are needed new motion–preserving treatments that, according to investigations have less (12%) risk of adjacent segments degeneration[27–29]. Moreover, the risks for symptomatic adjacent segment disease in motion–preserving procedures have been reported in 4.6%, significantly lower than patients that underwent intervertebral fusion[29].

One promising solution is disc arthroplasty (replacement), whose biomechanical objective is the restoration or preservation the mechanical functions of the disc[30]. This kind of replacement is divided mainly into two groups: nucleus prosthesis and total disc prosthesis. The latter one has been developed for more than 60 years, and in the specific case of lumbar arthroplasty only 3 of them have been approved by the U.S. Food and Drugs Administration (FDA)[31,32]. On the other hand, NP prostheses have been under investigation for fewer years, and none of them have achieved the FDA approval. These prostheses are designed to replace only the NP, maintaining the AF and the end plates intact, with the objective of restoring (indirectly) the biomechanical function of the entire IVD[30,33].

The development of NP replacement hence relies on the tissue engineering field, which focuses on the regeneration (using scaffolds) or replacement (using prosthesis) of damaged tissue[34]. In the case of scaffolds, it is believed that cells need a supporting material to act as template or substrate to attach and generate new tissue. In this scenario, highly porous structures are needed since they allow vascularization and diffusion of the nutrients and waste products. The tissue regeneration also depends on the pore size, since it has been demonstrated that a large surface area (higher inasmuch as smaller the pores) benefit cell attachmenl and growth, while a large pore size is also required to accommodate and deliver the sufficient cell mass for tissue regeneration, so an equilibrium in pore size should be attained[35]. Nevertheless, even with an optimum pore size, nutrients and cells migration will be inhibited without an interconnected pores structure. These morphology conditions promoted investigations in hydrogels, porous materials that in some cases like in Chitosan Hydrogels, have interconnective pores.

Another criterion to fulfill in prosthesis design is biocompatibility, and again, Chitosan hydrogels have demonstrated a good biocompatibility for IVD cells[36], antibacterial activity against a broad spectrum of bacteria and do not generate allergic or inflammatory responses after implantation, injection, ingestion or topical application[37–40]. Nonetheless, the problem with hydrogels is their low load–bearing capacity and their biocompatibility[3]. For those reasons, this investigation evaluated Chitosan–based hydrogels as a nucleus pulpous replacement, with several chemical variations to improve mechanical properties. First, the cross–linking with different Genipin concentrations. Genipin has been reported as a non–cytotoxic, anti–inflammatory, anti–angiogenic, anti–oxidative, antiproliferative, and apoptosis–inducing[41].

The second variation implemented for the CS based HGs was the insertion of two disperse phases and create and semi–interpenetrated networks hydrogel, using: Polyvinyl Alcohol (PVA) and Poly n–isopropylacrylamide (PNIPAm); in different proportions.

The study of NP replacements should assess mechanical, biocompatibility, bio–durability, cell–materials interaction and assimilation, kinematic testing, and safety testing; notwithstanding, this investigation focuses on the study of the first two characteristics in contrast with the NP properties.

Materials and methods
Materials
Chitosan MW 160.000 g/mol, deacetylation degree (DD) of 0,82±0,2 (measured by three different methods: Acid–Base Titration according to Youling et al.[42], UV–VIS Spectroscopy as stated by Renata et al.[43] and Fourier–transform infrared spectroscopy using Chitosan films and KBr pellets[44,45]); and NIPAm purity 97% were purchased from Sigma Aldrich. Genipin with a MW of 226 g/mol and purity≥98% was provided by Challenge Bioproducts, Polyvinyl Alcohol, MW 160.000 g/mol from Himedia was used. Acetic Acid (purity≥99,8%) from Fluca, and for the hemocompatibility test, Blood agar (base) from Merck and defibrinated blood from male sheep.

Methods
Chitosan/Genipin Stoichiometry Ratio
Having measured the Chitosan DD (0, 82), is fair to say that from every 100 monomers in the Chitosan chain, 82 monomers would correspond to D–glucosamine and 18 to N–Acetyl–Glucosamine. Thus, the molecular weight corresponding to 100 Chitosan monomers would be:

$$w_{100\ ChitosanMonomers} = \%DD * w_{Dglucosamine} + (100\% - \%DD) * w_{Nacetyl-Dglucosamine}$$

$$w_{100\ Chitosan\ Monomers} = 82x179,17gr + 18x221,21gr = 18673,72gr$$

This means that for each 18673g of Chitosan, 14692 g correspond to D–glucosamine or in other words, the percentage in weight of D–glucosamine in the Chitosan is 78,68%.

Since each Genipin molecule reacts with 2 D–glucosamine molecules to generate the cross–linking, for a 100% reaction of the D–glucosamine groups in the Chitosan, the Genipin amount necessary would be:

$$Genipinmol = 2\ xDglucosamine\ mol$$

But, since this study varied the Genipin percentage from 2,48%–5,4% (theoretically cross–linked percentage), to the former equation was needed to add a factor $0,0248 \leq n \leq 0,053$, resulting in the following equation:

$$Genipin\ mol = 2\ x\ Dglucosamine\ mol\ *n$$

In terms of molecular weight (MW), and replacing WD$_{glucosamine}$ in terms of Chitosan results:

$$W_{Genipin} = 2\ x\ \frac{W_{chitosan}x0,7868}{MW_{Dglucosamine}}\ x\ MW_{Genipin}$$

Hydrogels Preparation

The synthesis of PNIPAm has been previously published[46]. Three stock solutions were prepared; the first one of Chitosan 1,5% w/v in distilled water, with a concentration of 3% v/v of Acetic Acid. The second of PVA (3% w/v) in distilled water and the latter one of PNIPAm (2,5%w/v) also in distilled water. From these stock solutions, the different HGs formulations were prepared, see table 1.

Each formulation was firstly agitated in a vortex for 10 minutes and then poured in aluminum molds placed in a stove Precision Scientific model Thelco130, at 37°C (with vacuum) for 30h.
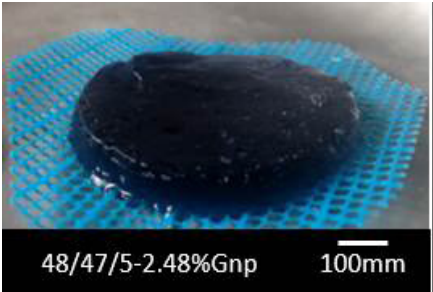
%CS	%PVA	%PNIPAm	%Genipin	Experimental Observation
48.0	47.0	5.0	2.480	
50.0	40.0	10.0	2.792	
54.0	45.0	1.0	3.281	
55.0	45.0	0.0	3.988	
68.0	24.0	8.0	4.058	
95.0	0.0	5.0	4.060	
100	0	0	2.480	
100	0	0	5.300	

48/47/5-2.48%Gnp   100mm

appearance of the gels synthesized; all the formulations presented the same shape

Table 1– Formulations subjected to different curing conditions.

Evaluation of solvent evaporation

First, an aluminum mold with only solvent (water with 3% Acetic Acid) was put into the stove at 37°C for 30h. Secondly, five HGs formulations were poured into different aluminum molds, covered with aluminum film (to avoid the solvent evaporation) and put into the stove at 37°C, also for 30h. In both cases the gelation was monitored (by visual evaluation of percolation). The five HGs formulations selected for this test were two from the lower edge of Chitosan proportion (48%) at the lower and higher Genipin percentage (2.48% and 5.3%); and two formulations from the higher Chitosan proportion (100%) at 3.92% and 2.85% of Genipin. and a formulation with an intermediate value of Chitosan (48%) and the presence of the two dispersed phases PVA and PNIPAm (47 and 5 % respectively). See table 2.

% CS	% PVA	% PNIPAm	% Genipin	Gelled after 30h?
48	52	0	2.48	No
48	52	0	5.30	No
48	47	5	2.71	No
100	0	0	2.48	Yes
100	0	0	5.30	Yes

Table 2 – Gelation of control samples averting solvent evaporation.

Swelling Study

After gelation, the HGs were subjected to lyophilization at −48°C and 0,1mBar for 48h in a lyophilizerLabconco model Freezona 2.5. The xerogels obtained, were weighed to obtain the dehydrated weight (w_0), followed by immersion in distilled water (pH 5,9±0,1) at 23°C for 96h. After that, they were weighed again to obtain the hydrated weight (wt) and with those values, the swelling ratio (SR) was measured[47].

$$S_R = \frac{w_t - w_0}{w_0}$$

Twenty three formulations were evaluated, where three of them were replicates and each formulation had also 3 repeated measures.

FT–IR Characterization

Before submerging the xerogels, samples were taken for infrared spectroscopy in a Thermo Scientific model iD3–ATR. Every xerogel was subjected to this study in the spectral region (4000–500) cm−1. Nonetheless, those samples with PNIPAm were studied before swelling and after swelling and lyophilization to study whether the interpenetrated phases were leaving from the Chitosan network.

Morphology evaluation

The xerogels were fractured using $N_{2(liquid)}$ and covered with a thin layer of gold through the sputtering process. After that, the samples were subjected to scanning electron microscopy (SEM) with a JOEL instrument model JSM–6390. In each SEM micrograph, approximately 100 pores were measured with the help of the Digimizer® program.

Rheological Characterization

To characterize viscoelasticity, an oscillatory shear test was carried out with a parallel plate rheometer brand TA instrument model AR2000. For this experiment, swelled hydrogels were placed in the rheometer chamber at 37°C, and a compressive strain of 10% (based on measured specimen thickness) was imposed on the discs for 2 minutes before rheological testing. Firstly, it was necessary to set up the constant strain for dynamic frequency sweep test, to ensure the study in the linear viscoelastic range, a strain sweep was performed. Once the linear viscoelastic region (LVR) of all samples was obtained, a (γ) strain common for all LVR (0.2%) was selected to carry out the dynamic frequency sweep test from 0.1rad/sec to 100 rad/sec. The samples studied in this experiment were the swelled samples from the swelling study.

Hemolysis Test

In these experiments, the S–IPN HGs were put in contact with a blood agar solution to evaluate the hemolytic properties of those materials. Nonetheless, this enriched medium also enhances bacteria growth, altering the study of the material biocompatibility, making the sterilization of all equipment and samples previous to the essay necessary. To sterilize Petri dishes and eppendorfs that would be in contact with the samples and the agar–blood solution, they were put in an autoclave, at 120°C and 1.2psi for 2 hours. To sterilize the xerogels, they were put in the sterilized eppendorfs with a 75% ethanol solution. Those eppendorfs were then placed uncovered inside a UV (enclosed and sterilized) chamber for 24h (allowing the ethanol solution to evaporate). On the other hand, the agar–blood solution was prepared, and under sterile conditions, the medium and each sample were transferred to the sterile Petri dishes and incubated at 37°C with a 5%CO2 flow. The areas around the hydrogels were observed after 24h and 48h and digital pictures(8MP) for further comparison with the control sample (agar–blood medium). In this experiment, toxicity was indicated by a loss of viable cells around the test device, perceptible by a color change around the sample. A lack of hemolysis (sometimes called γ hemolysis) was indicated when the zone surrounding the sample was indistinct from the rest of the agar–blood. A greenish to brownish discoloration of the medium was a sign of oxidation [48,49].

Statistical Analyses

This investigation established a constant concentration of polymers in the initial formulations of 1.5% w/v. Within that polymer's concentration, a variation of proportions in the polymers´ components were also established according to table 1.

The Genipin concentration, on the other hand, was studied between 2.48 and 5.4%. In these ranges of mixture components (CS, PVA, and PNIPAm) and numerical factor (Genipin), a design of experiment was carried out using the tool Combined DOE of the program DesignExpert® with a D–Optimally design.

After synthesis and characterization, an analysis of the empirical data obtained from swelling and rheology test were made. First, a normalization of data through Box–Cox transformation[50] was needed and secondly, the statistical model selection was made taking into account Akaike's information criterion (AICc), p–value, model lack of fit, model precision and the difference between $r^2_{predicted}$ and $r^2_{adjusted}$ [51].

Results and Discussion
Gelation

During the gelation process a decrease in the solution volume of almost all mixtures was observed. This was supported by the decrease in the solution volume of the 100% solvent sample. Because of the solvent evaporation, it is worth mentioning that this concludes in an increment of the solute concentration (polymers and cross–linked).

Regarding the synthesis, Table 2 shows that for samples with 100% of CS, regardless of the Genipin percentage the formulations percolated the mold (even those with the smallest Genipin%). In contrast, formulations with 48% of CS did not attain percolation, not even with the higher Genipin percentage. For these cases, the cure time was greater than 48 hours.

This implies that the critical variable responsible of gelation in less than 30h was the Chitosan proportion. This makes sense since the Chitosan/Genipin system is solely responsible for generating a macromolecule able to percolate all the system (since these two components are the only ones forming chemical bonds)[52–55]. Furthermore, the stoichiometric ratio between CS–Genipin implies that an increment in the Chitosan proportions increments the Genipin concentration in the solution.

Secondly, it could be seen that samples with low Chitosan proportions did not percolate before 30h. The hypotheses that can explain this behavior is that in the formulations with smaller CS amount, this concentration could have been too small to percolate the entire system (to attain sol–gel transition). In that way, allowing solvent evaporation in the system increases the solute concentration up to the point in which the CS/Genipin concentration would be enough to percolate (besides of the five samples during the experiment of "evaluation of solvent evaporation" all the other samples were synthesized uncovered and allowing the solvent evaporation). Furthermore, it has been reported that diminishing the system responsible of gelation (CS/GNP) decreases the kinetic[56] reaction, and the introduction of PVA phase slows down the cross–linking reaction between CS and GNP[57].

Hydrogels structure

From FT–IR the first sign of the Genipin presence in the hydrogels structure was the absorption of the internal double bonds of the Genipin–cyclopentane. This might be responsible for the absorption band in 1540cm^{-1} (Figure 1). Regularly, unconjugated alkenes show moderate to weak absorption at 1667 cm^{-1}– 1640cm^{-1} but in the case of cycloalkenes, the C=C stretch vibration is coupled with the C–C stretching of the adjacent bounds, interaction that diminishes inasmuch as the angle within the cycloalkene decrease up to 90° displacing the absorption band to the right[58].

A second sign of the Genipin presence in the hydrogels was the absorption bands in 795 cm^{-1} and 1410cm^{-1}, where they correspond to the C–H out–of–plane bending vibrations of the Genipin´s alkenes[58,59].

Regarding the HGs with a PVA phase, most of the bands in this polymer´s spectrum were already in the Chitosan, so, the only difference in

the spectrum that allowed the verification of PVA presence in the HGs was the band 1720 cm^{-1} (Figure 2.a), which was sign of the absorption of the residuals acetate groups during the manufacturing of PVA from hydrolysis of polyvinyl acetate[60,37].

The hydrogels with an interpenetrated network of PNIPAm also overlapped all its bands with the Chitosan HGs bands, since they had the same functional groups. Nonetheless, it was possible to observe a sharper band in 1260cm^{-1} in contrast with the rest of the bands in the hydro−gels spectrum (Figure,2.b) consequence of the increment in the methyl groups presents in the PNIPAm.
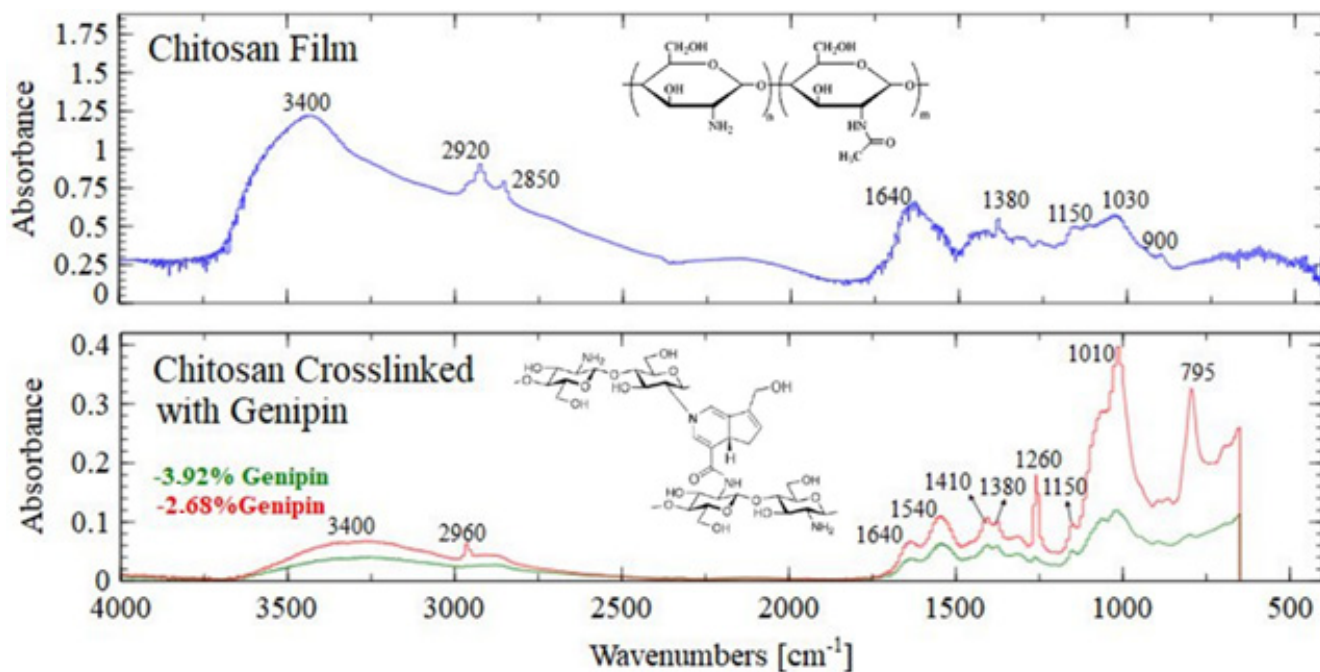
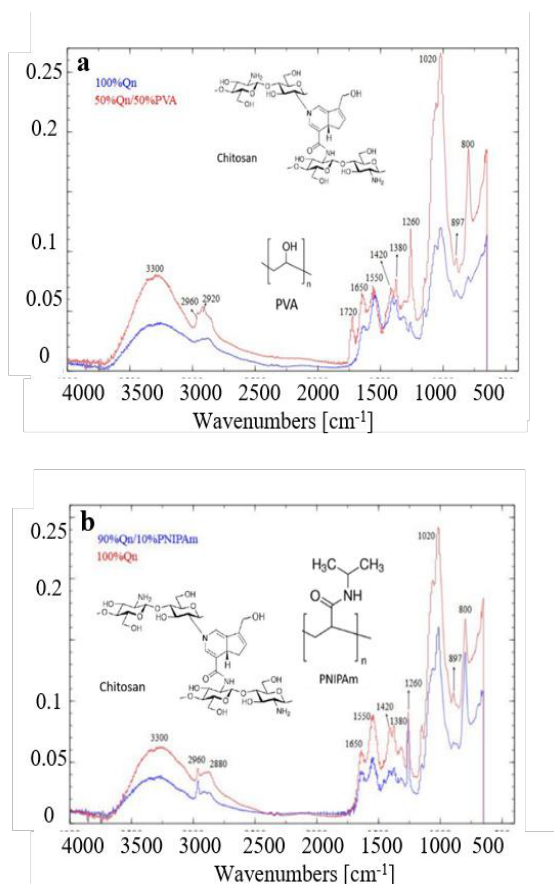**Figure 1 −** FTIR Spectra of Chitosan Film and HGs of 100% Chitosan with 3.92 and 2.68% of Genipin.

Figure 2 − a) FTIR Spectra of Chitosan HG and Chitosan/PVA HG. b) FTIR Spectra of Chitosan HG and Chitosan/PNIPAm HG.

Hydrogels morphology

Variation in the Genipin percentage allowed the modification in the pore size distribution (figure 3−a). In this figure you can see that a de−crease in the Genipin percentage narrowed the pore size distribution of the HGs, and furthermore it diminished the pore size[57,58].

Theoretically, an increment in the Genipin concentration augments the cross−linked density[59], this might be the cause of the increment in the pore´s wall thickness (figure 3−b).

Regarding the polymers composition variation, a diminishing in the Chitosan proportion generated an increment in the wall thickness and a decrement in the pore size (Figure 4). This was a consequence (as before mentioned) of a lessening in the components responsible for the gelation, which augmented evaporation of the solvent producing a densification of the solution.

Another relevant feature in the HGs microstructure was the highly porous and interconnective structure obtained in all HGs.
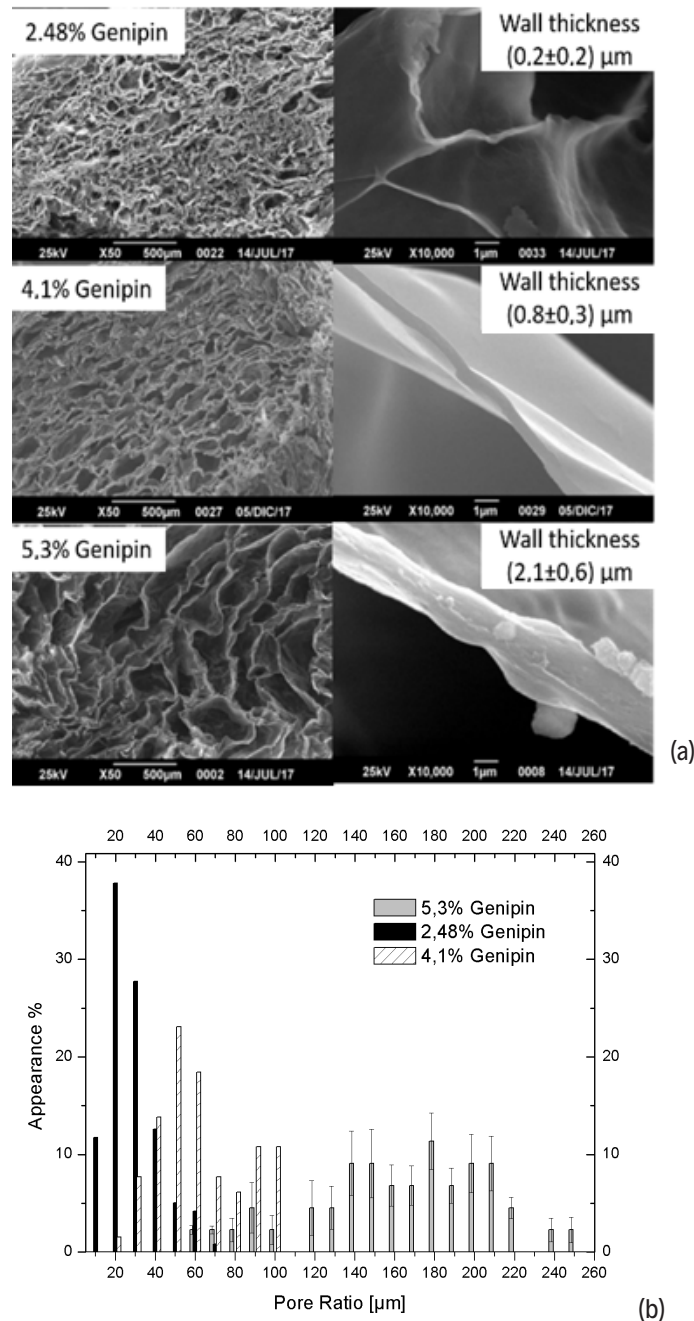

Figure 3 − Hydrogels with different Genipin concentration and the same polymers composition (48% Chitosan, 47% PVA and 5% PNIPAm): (a) Cross section SEM micrographs. (b) Pore ratio distribution (obtain from SEM micrographs).
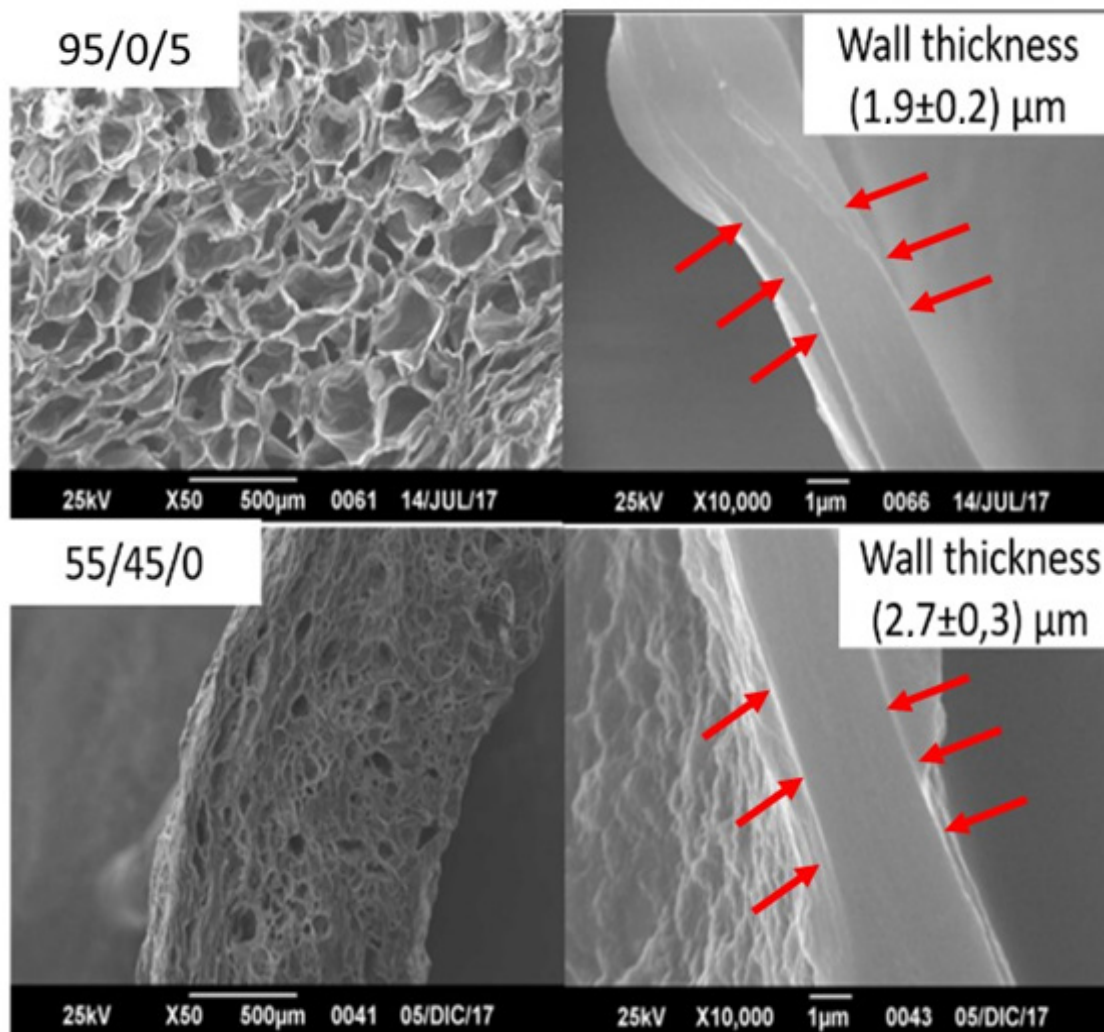
Figure 4. Cross section SEM micrographs: S−IPN Hydrogels with different polymers proportions and the same Genipin concentration (~4 %).

HGs Swelling Study

The statistical model that better fitted the experimental data was represented by the follow equation:

$$SR = 0.26xCS + 4.58xPVA + 0.54xPNIPAm − 0,07xCSxPVA − 1.74xPVAxGNP$$

(equation 1)

Where SR is the swelling ratio this model had a p−value of 1,4E^{-7}, with a lack of fit of 0.36, r^2 of 0.941582 (with $r^2_{predicted}$−$r^2_{adjusted}$=0,02) and an adequate precision of 23.7.

The first three terms indicate that PVA, PNIPAm, and CS produced an increment in the SR of the HGs. In the case of PVA, it makes sense because of its hydrophilic nature [60]. Regarding Chitosan, this was no surprise either since the distilled water had a smaller pH than the Chitosan´s pKa, allowing primary amine groups to be protonated and promoting counter ions (water molecules) to migrate from the surrounding medium to the inside of the HG resulting in an osmotic pressure difference. This process is named Donnan equilibrium[42,54,61]. Results are shown in figure 5.

In the same way, PNIPAm at the temperature of the medium (24°C) was below the lower critical solution temperature (LCST) which implies a linear structure and hydrophilic behavior in this polymer[62,63].

Even when the lack of strong physical or chemical bonds between PNIPAm and the other phases at temperatures below LCST has been reported as allowing a leakage of this polymer from the S−IPN structure towards the fluid[62], this was not the case, since the study of the char−acteristic band (1260cm^{-1}) obtained in the FTIR essay of a xerogel (containing PNIPAm) and then after swelling and lyophilization of the same sample, showed no change in the intensity of that band. This is possible because the physical entanglement between the S−IPN and the chitosan network.

The phenomenon of swelling mentioned before deals only with water type I and II [63,64]. For water type III (also called interstitial water) is necessary to consider the HG pore size since the water type III locates in the free space inside the HG´s structure[65]. Thus, while smaller pores hold a smaller amount of water type III in the structure, that might be the reason for the decrease of the SR inasmuch as the GNP percentage diminished. Figure 4 shows graphically the effect of the polymers proportion over the SW in the upper and lower edges of Genipin concentration.
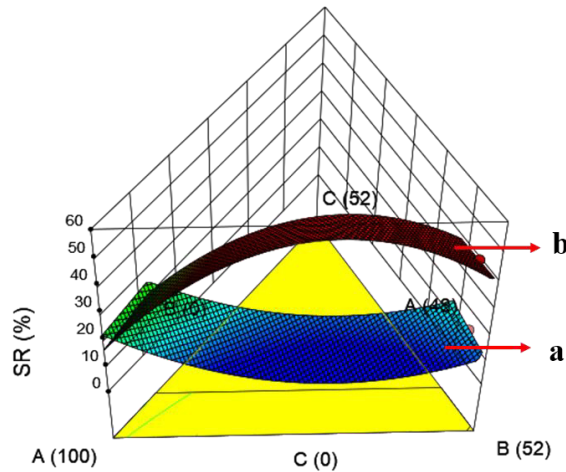
Figure 5 − Effect of the polymers proportion over the swelling ration in the: (a) lower (2.48%) and (b) upper (5.4%) edges of Genipin concentration. With A, B and C are CS, PVA and PNIPAm proportions respectively.

Mechanical properties

In the case of the storage modulus (G´) the statistical model that better fitted the experimental data was represented by the following equation:

$$\sqrt{G'} = 2.32xCS + 14.45xPVA + 1.36xPNIPAm - 5.90xPVAxGNP$$

(equation 2)

This model had a p−value smaller than 0.0001 with a lack of fit of 1.91, r^2 of 0.91 (with $r^2_{predicted} - r^2_{adjusted} = 0,07$) and an adequate precision of 17.68.

The PVA effect showed an increment of G´ inasmuch as the Genipin percentage diminished the concentration (Figure 6). The first explanation for this outcome relies on the fact that increasing the amount of SR decreases the elastic modulus (and other mechanical properties)[54,66−68], hence, those components that diminished the structure pore size, reduce the SR, producing an increment in the storage modulus (which is the case of diminishing Genipin percentage and augmenting PVA proportion)[69]. Secondly, knowing that a uniform pore structure also improves the mechanical properties of the HG[70], increasing PVA proportion and diminishing the Genipin concentration, narrows the range of pore size increasing the storage modulus. Third, it has also been reported that an S−IPN of PVA endows the Chitosan network of stiffness owing to the hydrogen bonds between these two polymers[54]. And fourth, even when theoretically, increasing the amount of cross−linking agent, increases the cross−linking density concluding in an improvement of mechanical properties[68], it has been reported that when the cross−linking overcomes a threshold, highly cross−linked heterogeneities appear, resulting in a diminishing in the number of cross−links formed and then in the mechanical properties[68]. Low et al. located that threshold for CS hydrogels cross−linked with GNP in 1% w/v of Genipin[57], which agrees with this investigation, where G´ decreased inasmuch as the Genipin concentration rose from 2,48% to 5,4%. Finally, the effect of PNIPAm over G´ was not that relevant in contrast with the effect of PVA and Genipin, nonetheless, it is reasonable to expect an increment in G´ since the PNIPAm at 37°C is contracted due to a collapse of the polymer coil, diminishing the SR of the HG[69−71].

Regarding the lag between stress and strain (δ), the models tested in the statistical analysis did not give reliable information owing to the lack of fit of models and the difference between $r^2_{predicted}$ and $r^2_{adjusted}$ which was greater than 0,2 in all cases.
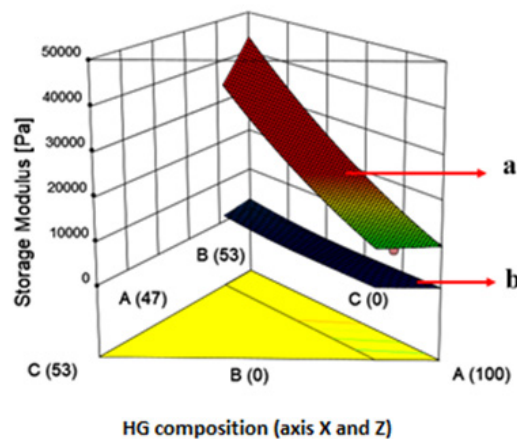

Figure 6 − Effect of the polymers proportion over the Storage modulus in the: (a) lower (2.48%) and (b) upper (5.4%) edges of Genipin concentration. With A, B and C are CS, PVA and PNIPAm proportions respectively.

Applications of S−IPN HGs as materials for NP replacement

Table 3 shows G´ and loss tangent (tanδ) for Nucleus pulpous according to different investigations[5, 73, 74], as well as those values for the HG S−IPN synthesized in this investigation, specifically those with the highest and smallest mechanical properties.

From table 3 it can be depicted that G´ of the S−IPN HG could be tailored to NP´s G´, nonetheless, the value of tanδ was always smaller than the NP´s corresponding value, this means, the S−IPN HG behaved more like an elastic solid than NPs.

Ideally, a NP replacement should guarantee a minimally invasive surgery, looking forward to maintaining the integrity of the annulus fibrosus and end plates; hence, the best option is the injection of the implant into the disc space for in situ healing. Despite that in the S−IPN HG process of gelation they suffered a process of solvent evaporation, further studies are needed to figure out if these HGs can be synthetized allowing evaporation process just before the sol−gel transition (when the solution still flows) but prevented after that point, looking forward to the solution injection before sol−gel transition to in situ healing and still obtaining the S−IPN HG.

The effect over tissue regeneration, shelf life, and degradability of this S−IPN HGs should also be studied to figure out if they are suitable as a prosthesis or as a scaffold. Nonetheless, this investigation proved that the pore morphology can be controlled by modifying the components proportions and crosslinking percentage, feature that can be tailored to improve the process of tissue regeneration, since a more uniform pore size facilitates the spatial distribution of fibroblasts, differentiation of preosteoblasts and diffusion of macromolecules, leading to even distribution of cells and homogeneous differentiation of cells[59,75].

G´[kPa]	tanδ	Source	Species
20.8	0.28	[73]	Goats
0.32	0.26	[74]	Porcine
4.7-26.5	0.38-0.53	[5]	Human L4-L5
27.96	0.045	*	HG S-IPN
0.077	0.23	**	HG S-IPN

Where * represents the formulation 50/40/10 and 2.8%GNP and ** the formulation 95/0/5 and 4.1%GNP.

Table 3 − Comparison between rheological properties of NP and S−IPN HGs.

Hemocompatibility

Blood is composed of 90% to 95% of water and around 5% of cells (red blood cells, white blood cells, platelets, etc.)[71]. A toxic material could generate hemolysis, which is the rupture of the cellular membrane of the red blood cells killing the cell[43,44]. Every S−IPN HG formulation does not exhibited hemolysis (no appearance of a whitish halo around the samples), a sign of a none−cytotoxic feature, asseveration that can be extrapolated to HGs in the whole range of Genipin percentage and polymers proportions studied[72]. See figure 7 for hemocompatibility results.
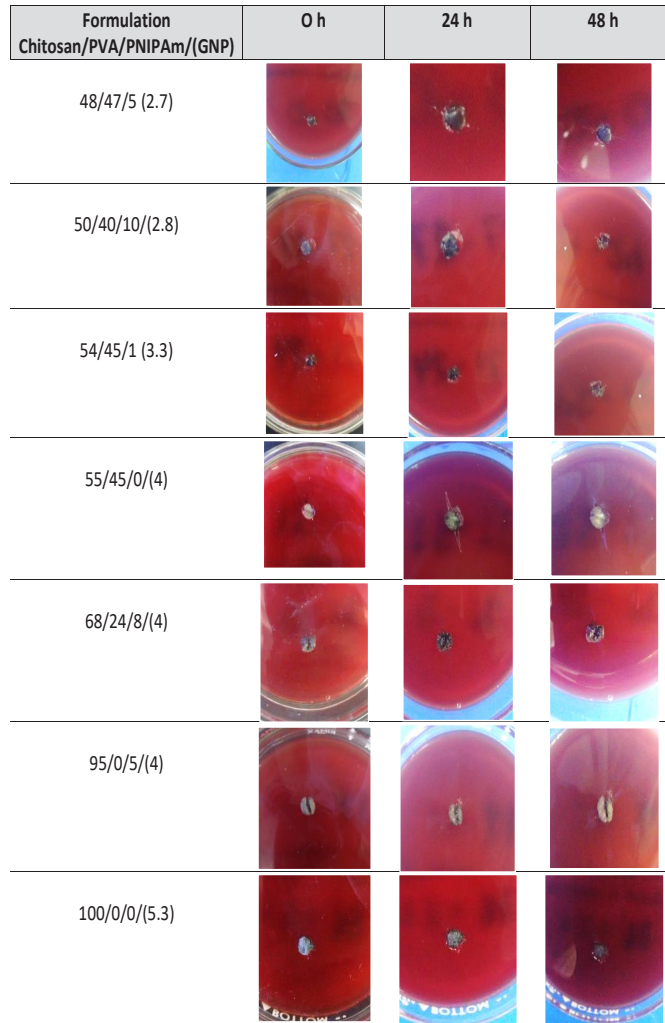
Formulation Chitosan/PVA/PNIPAm/(GNP)	0 h	24 h	48 h
48/47/5 (2.7)			
50/40/10/(2.8)			
54/45/1 (3.3)			
55/45/0/(4)			
68/24/8/(4)			
95/0/5/(4)			
100/0/0/(5.3)			

Figure 7− Hemocompatibility of agar/ blood gel formulations Evolution for 48 hr at 37°C.

Conclusions

Modification in CS/PVA/PNIPAm proportion and GNP percentage can control the pore size and its size distribution, the SR and the storage modulus.

The range of storage modulus obtained by the different S−IPN HGs studied, agree with the values for the storage modulus of human lumbar NPs and other species. Meanwhile, the loss tangent achieved in S−IPN HGs were also close to NPs values. These outcomes alongside with its non−cytotoxic feature, stand up this kind of S−IPN HGs for further study as material for NP prosthesis

Acknowledgment

References

[1]. Qi−Bin Bao, Geoffrey M. Mccullen, Paul A. Higham, John H. Dumbleton and Hansen A.Yuan "Review: The artificial disc: theory, design and materials" Biomaterids , Vol. 17, pp. 1157−1167, 1996.

[2]. C. Jongeneelen, Biomechanics in the intervertebral disc, A literature review, Eindhoven: University of Technology, pp 1−15, 2006.

[3]. Chan, S. C. y B., Gantenbein Ritter "Intervertebral disc regeneration or repair with biomaterials and stem cell therapy − feasible or fiction?" Swiss Med Weekly, vol. 142, pp. 1−12, 2012.

[4]. Iatridis JC1, Nicoll SB, Michalek AJ, Walter BA, Gupta MS. "Role of biomechanics on intervertebral disc degeneration and regenerative therapies: What needs repairing in the disc and what are promising biomaterials for its repair?" Spine Journal, vol. 13, n° 3, p. 243−262, 2013.

[5]. Iatridis, James C.; Weidenbaum, Mark; Setton, Lori A.; Mow, Van C., "Is the nucleus pulpous a solid or a fluid? Mechanical behaviors of the

nucleus pulpous of the human intervertebral disc" Spine, vol. 21, n° 10, pp. 1174–1184, 1996.

[6]. Nikolai Bogduk, "Clinical Anatomy of the Lumbar Spine and Sacrum", London/New York/ Oxford/Philadelphia/St Louis/Sydney/Toronto: Elsevier, pp. 1–77, 2005.

[7]. Zhiyu Zhou, Manman Gao, Fuxin Wei, Jiabi Liang, Wenbin Deng, Xuejun Dai, Guangqian Zhou and Xuenong Zou, "Shock Absorbing Function Study on Denucleated Intervertebral Disc with or without Hydrogel Injection through Static and Dynamic Biomechanical Tests In Vitro" BioMed Research International, pp. 1–7, 2014.

[8]. Irving M. Shapiro and Makarand V., "The Intervertebral Disc", Philadelphia: Springer, pp.3–52, 109–124 and 139–170, 2014.

[9]. Peter J. Roughley, "Biology of intervertebral disc aging and degeneration: Involvement of the extracellular matrix" Spine, vol. 29, n° 23, pp. 2691–2699, 2004.

[10]. James N. Parker, and Philip M. Parker, "Degenerative Disc Disease", San Diego: ICON Health Publications, 2004.

[11]. D.W., Meakin J.R. and Hukins, "Effect of removing the nucleus pulpous on the deformation of the annulus fibrosus during compression of the intervertebral dis" Biomechanics, vol. 33, n° 5, pp. 575–580, 2000.

[12]. Manohar Panjabi, Mark Brown, Sven Lindahl, Lars Irstam, and Martin Hermens, "Intrinsic disc pressure as a measure of integrity of the lumbar spine" Journal Spine, vol. 13, n° 8, pp. 913–917, 1988.

[13]. Richard E. Seroussi, Martin H. Krag, David L. Muller and Malcolm H. Pope, "Internal deformations of intact and denucleated human lumbar discs subjected to compression, flexion, and extension loads" Orthopaedic Research, vol. 7, n° 1, p. 122–131, 1989.

[14]. Iatridis JC, Setton L.A., Weidenbaum M., Mow V.C., "Alterations in the mechanical behavior of the human lumbar nucleus pulpous with degeneration and aging" J Orthop Res., vol. 15, n° 2, pp. 318–322, 1997.

[15]. Brinkman P, Grootenbore H. ,"Change of disc height, radial disc bulge and intradiscal pressure from discectomy" Spine, vol. 16, pp. 641–646, 1991.

[16]. Nishiyama K, Nye T., "Kinematics of whole lumbar spine, effect of discectomy" Spine, vol. 10, pp. 543–554, 1985.

[17]. Michael A. Adams, "Biomechanics of back pain" Acupuncture in Medicine, vol. 22, n° 4, pp. 178–188, 2004.

[18]. Simon Dagenais, Jaime Caro, and Scott Haldeman "A systematic review of low back pain cost of illness studies in the United States and internationally" The Spine Journal, vol. 8, pp. 8–20, 2008.

[19]. Surgeons, American Academy of Orthopaedic "The Burden of Musculoskeletal Diseases in the United States," Rosemont, IL: Bone and Joint Decade, 2008. Available: http:// www.boneandjointburden.org/.

[20]. Jensen M.C., Kelly A.P., Brant–Zawadzki M.N., "MRI of degenerative disease of the lumbar spine" Magn Reson Q., vol. 10, n° 3, p. 173–190, 1994.

[21]. Shono Y., Kaneda K, Abumi K., "Stability of posterior spinal instrumentation and its effects on adjacent motion segments in the lumbosacral spine" Spine, vol. 23, pp. 1550–1558, 1998.

[22]. Lehman T. R., Spratt K. F., "Long–term follow–up of lower lumbar fusion patients" Spine, vol. 12, pp. 97–104, 1987.

[23]. Lee C. K. and Langrana N. A., " Lumbosacral spinal fusion: a biomechanical study" Spine, vol. 9, pp. 574–581, 1984.

[24]. O'Connell G.D., Malhotra N.R., Vresilovic E.J., Elliott D.M., "The Effect of Discectomy and the Dependence on Degeneration of Human Intervertebral Disc Strain in Axial Compression" Spine, vol. 36, n° 21, p. 1765–1771, 2011.

[25]. Judith R. Meakin, Thomas W. Redpath, David W.L. Hukins, "The Effect of Partial Removal of the Nucleus Pulpous from the intervertebral Disc on the Response of the Human Annulus Fibrous to Compression" Clinical Biomechanics, vol. 16, pp. 121–128, 2001.

[26]. Neil R. Malhotra, Woojin M. Han, Jesse Beckstein, Jordan Cloyd, "An Injectable Nucleus Pulpous Implant Restores Compressive Range of Motion in the Ovine Disc" Spine, vol. 37, n° 18, p. 1099–1105, 2013.

[27]. Gillet P., "The fate of the adjacent motion segments after lumbar fusion" J Spinal Disorder Tech, vol. 16, n° 4, pp. 338–45, 2003.

[28]. Rahm M.D., Hall B.B., "Adjacent segment degeneration after lumbar fusion with instrumentation: a retrospective study" Spinal Disorder., vol. 9, n° 5, pp. 392–400, 1996.

[29]. Chunpeng Ren, Yueming Song, Limin Liu, Youdi Xue, "Adjacent segment degeneration and disease after lumbar fusion compared with motion−preserving procedures: a meta−analysis,» Orthop Surg Traumatol, vol. 24, n° 1, p. 245−253, 2014.

[30]. Casey K. Lee, Vijay K. Goel, "Artificial disc prosthesis: design concepts and criteria" The Spine Journal, vol. 4, pp. 209−218, 2004.

[31]. Aetna, "Intervertebral Disc Prostheses" 17/01/2018. Available: http://www.aetna.com/cpb/medical/data/500_599/0591.html.

[32]. Angelo Carpy, "Progress in Molecular and Environmental Bioengineering − From Analysis and Modeling to Technology Applications", Rijeka, Croatia, InTech, 2011, pp. 117−150.

[33]. Hassan Serhan, Devdatt Mhatre, Henri Defossez, "Motion−preserving technologies for degenerative lumbar spine: The past, present, and future horizons" SAS Journal , vol. 5, pp. 75−89, 2011.

[34]. Raphael M. Otternbrite, Kinam Park, Teruo Okano "Biomedical Applications of Hydrogels Handbook", New York−London: Springer, pp 227−242.

[35]. Shoufeng Yang, Kah−Ah−Fai Leong, Zhaohui Du y Chee−Kai Chua, "The Design of Scaffolds for Use in Tissue Engineering. Part I. Traditional Factors" Tissue Engineering, vol. 7, n° 6, pp. 679−689, 2001.

[36]. Cheng Y.H., Yang S.H., Su W.Y., Chen Y.C., Yang K.C., Cheng W.T., Wu S.C., Lin F.H., "Thermosensitive chitosan−gelatin− glycerol phosphate hydrogels as a cell carrier for nucleus pulpous re− generation: an in vitro study" Tissue Eng. Part A. , vol. 16, n° 2, pp. 695−703, 2010.

[37]. Youling Yuan, Betsy M. Chesnutt, Warren O. Haggard and Joel D. Bumgardner, "Deacetylation of Chitosan: Material Characterization and in vitro Evaluation via Albumin Adsorption and Pre−Osteoblastic Cell Cultures" Materials, vol. 4, pp. 1399−1416, 2011.

[38]. Renata Czechowska−Biskup, Diana Jarosińska, Bożena Rokita, Piotr Ulański, Janusz M. Rosiak, "Determination of Degree of Deacetylation of Chitosan − Comparison of methods" Progress on chemistry and application of chitin and its derivatives, vol. 17, pp. 5−20, 2012.

[39]. Mad Rabiul Hussain, Murshid Iman and Tarun K. Maji, "Determination of Degree of Deacetylation of Chitosan and Their effect on the Release Behavior of Essential Oil from Chitosan and Chitosan− Gelatin Complex Microcapsules" Advanced Engineering Applications, vol. 2, n° 4, pp. 4−12, 2013.

[40]. Tanveer Ahmad Khan Kulliyyah, Kok Khiang Peh, Hung Seng Chang "Reporting degree of deacetylation values of chitosan: the influence of analytical methods" Pharm Pharmaceut Sci., vol. 5, n° 3, pp. 205−212, 2002.

[41]. Maria G. Carrero, James J. Posada, Marcos A. Sabino "Intelligent Copolymers Based on Poly (N−Iopropylacrylamide) PNIPAm with potential use in Biomedical Applications. Part. I PNIPAm Functionalization with 3−Butenoic Acid and Piperazine" International Journal of Advances in Medical Biotechnology, vol. 1, n° 1, pp. 1−8, 2018.

[42]. Steve Rimmer, "Biomedical Hydrogels, Oxford, Cambridge, Philadephia and New: Woodhead Publishing, pp. 35−61, 2011.

[43]. Brian J. Tindall, Johannes Sikorski, Robert A. Smibert, and Noel R. Krieg "Phenotypic Characterization and the Principles of Comparative Systematics" de Methods for General and Molecular Microbiology, Washington, ASM Press, 2007, pp. 335−386.

[44]. Encyclopedia, "World of Microbiology and Immunology", Available: https://www.encyclopedia.com/science/encyclopedias−almanacs−transcripts−and−maps/blood−agar−hemolysis−and−hemolytic−reactions. [last access: 7/4/2018].

[45]. G. P. Box and D. R. Cox, "An Analysis of Transformations" Research Methods Meeting of the Society, pp. 211−252, 1964.

[46]. Kenneth P. Burnham and David R. Anderson, "Model Selection and Multimodel Inference: A Practical Information− Theoretic Approach", Berlin, Heidelberg, Barcelona, Hong Kong, London, Milan and Paris: Springer, pp. 49−65 y 98−121. 2002.

[47]. A. Carpi, "Progress in Molecular and Environmental Bioengineering − From Analysis and Modeling to Technology Applications", InTech, pp. 117−141. 2011.

[48]. John K. Gillham, "Formation and Properties of Thermosetting and High Tg Polymeric Materials" Polymer Engineering and Science, vol. 26, n° 20, pp. 1429−1433, 1986.

[49]. H. S. V. y. R. J. W. Jean Pierre Pscault, Thermosetting Polymers, New York: Marcel Dekker, pp. 1−10. 2002.

[50]. M. José Moura, M. Margarida Figueiredo y M. Helena Gil, "Rheological study of genipin cross−linked chitosan hydrogels" Biomacromolecules, vol. 8, pp. 3823−3829, 2007.

[51]. George Odian, "Principles of Polymerization" New York, John Wiley & Sons, 2004, pp. 39−50.

[52]. Nand A.V., Rohindra D.R. y Khurma, J.R., "Characterization of genipin crosslinked hydrogels composed of chitosan and partially hydrolyzed

poly(vinyl alcohol)" E-Polymers, pp. 30–38, 2007.

[53]. Robert M. Silverstein, Francis X. Webster, David J. Kiemle "Spectrometric identification of organic compounds", New York: John Wiley & Sons, 81–90. 2005.

[54]. Tao Wang, Mahir Turhan and Sundaram Gunasekaran "Selected properties of pH-sensitive, biodegradable chitosan–poly(vinyl alcohol) hydrogel" Polymer International, vol. 53, pp. 911–918, 2004.

[55]. A. M. Shehap, "Thermal and Spectroscopic Studies of Polyvinyl" Egypt. J. Solids, vol. 31, n° 1, 2008.

[56] .Christie M. Hassan, and Nikolaos A. Peppas, "Structure and Applications of Poly(vinyl alcohol) Hydrogels Produced by Conventional Crosslinking or by Freezing/Thawing Methods" de Biopolymers PVA Hydrogels, Anionic Polymerization Nanocomposites, Berlin Heidelberg, Springer-Verlag, 2000, pp. 37–65.

[57]. Long Bi, Zheng Cao, Yunyu Hu, Yang Song, Long Yu, Bo Yang, Jihong Mu, Zhaosong Huang y Yisheng Han, "Effects of different cross-linking conditions on the properties of genipin-cross-linked chitosan/collagen scaffolds for cartilage tissue engineering" J Mater Sci: Mater Med, vol. 22, pp. 51–62, 2011.

[58]. Simona Dimida, Amilcare Barca, Nadia Cancelli, Vincenzo De Benedictis, Maria Grazia Raucci, y Christian Demitri, "Effects of Genipin Concentration on Cross-Linked Chitosan Scaffolds for Bone Tissue Engineering: Structural Characterization and Evidence of Biocompatibility Features" International Journal of Polymer Science, pp. 1–7, 2017.

[59]. Jiabing Ran, Lingjun Xie, Guanglin Sun, Jingxiao Hu, Si Chen, Pei Jiang, Xinyu Shen, Hua Tong "A facile method for the preparation of chitosan-based scaffolds with anisotropic pores for tissue engineering applications" Carbohydrate Polymers, vol. 152, p. 615–623, 2016.

[60]. Tayser Sumer Gaaz, Abu Bakar Sulong, Majid Niaz Akhtar, Abdul Amir H. Kadhum, "Properties and Applications of Polyvinyl Alcohol, Halloysite Nanotubes and Their Nanocomposites" Molecules, vol. 20, p. 22833–22847, 2015.

[61]. Sundaram Gunasekaran, Tao Wang, Chunxiang Chai, "Swelling of pH-Sensitive Chitosan-Poly(vinyl alcohol) Hydrogels" Journal of Applied Polymer Science, vol. 102, p. 4665–4671, 2006.

[62]. Mingzhen Wang, Yu Fang , Daodao Hu "Preparation and properties of chitosan–poly(N-isopropylacrylamide) full-IPN hydrogels" Reactive & Functional Polymers, vol. 48, pp. 215–221, 2001.

[63]. Kamiya Jain, Raman Verdarajan, Masaki Watanabe, Masaki Ishikiriyama, and Noriyoshi Matsumi, "Tunable LCST behavior of poly(N-isopropylacrylamide/ionic liquid) copolymers" Polymer Chemistry, n° 38, pp. 6819–6825 , 2015.

[64]. I. G. Pedley and B. J. Tighe, "Water Binding Properties of Hydrogel Polymers for Reverse Osmosis and Related Applications" Brit. Polym., vol. 11, pp. 130–136, 1979.

[65]. Hossein Omidian and Kinam Park, "Introduction to Hydrogels" de Biomedical Applications of Hidrogels Handbook, New York, Dordrecht, Heidelberg and London, Springer, 2010, pp. 1–15.

[66]. Victor T. Wyatt, "Effects of Swelling on the Viscoelastic Properties of Polyester Films Made from Glycerol and Glutaric Acid" Journal of Applied Polymer Science, vol. 1, pp. 1–10, 2012.

[67]. H. Bendaikha, S. Chaoui, S. Ould Kada, and A. Krallafa,"Swelling behavior and viscoelastic properties of a Polyacetal Hydrogel" AIP Conference Proceedings, vol. 64, 2008.

[68]. Kristi S. Anseth, Christopher N. Bowman and Lisa Brannon-Peppas, "Mechanical properties of hydrogels and their experimental determination" Biomaterials, vol. 17, pp. 1647–5167, 1996.

[69]. Hye Yun Kim, Ha Neul Kim, So Jin Lee, Jeong Eun Song, Soon Yong Kwon, Jin Wha Chung, Dongwon Lee and Gilson Khang,"Effect of pore sizes of PLGA scaffolds on mechanical properties and cell behavior for nucleus pulpous regeneration in vivo" Tissue Engineering and Regenerative Medicina, vol. 11, n° 1, pp. 44–57, 2014.

[70]. Jorge M. Sobral, Sofia G. Caridade, Rui A. Sousa, João F. Mano, "Three-dimensional plotted scaffolds with controlled pore size gradients: Effect of scaffold geometry on mechanical performance and cell seeding efficiency" Acta Biomaterialia, vol. 7, pp. 1009–1018, 2011.

[71]. Laxman S. Desai and Laurence Lister, "Biocompatibility Safety Assessment of Medical Devices: FDA/ISO and Japanese Guidelines" Toxikon Corp., pp. 1–19, 2016.

[72]. Marta A. Cooperstein and Heather E. Canavan, "Assessment of cytotoxicity of (N-isopropyl acrylamide) and Poly (N-isopropyl acrylamide) coated surfaces" Bio interphases, vol. 8, n° 19, pp. 1–12, 2013.

[73]. J.L. Bron, G.H. Koenderink, V. Everts, T.H. Smit, "Rheological Characterization of the Nucleus Pulposus and Dense Collagen Scaffolds Intended for Functional Replacement" Journal of Orthopedic Research, pp. 620–626, 2009.

[74]. F. Causa, L. Manto, A. Borzacchiello, R. De Santis, P. A. Netti, L. Ambrosio, L Nicolais, "Spatial and Structure Dependence of Mechanical Properties of Porcine Intervertebral Disc" Journal of Material Science: Materials in Medicine, vol. 13, pp. 1277−1280, 2002.

[75]. Sung−Wook Choi, Yu Zhang y Younan Xia, "Three−dimensional Scaffolds for Tissue Engineering: The Importance of Uniformity in Pore Size and Structure" Langmuir, vol. 26, nº 24, p. 19001−19006, 2010.